NASA/TM—2003-212723 ARL–TR–3091

Adaptive Detuning of a Multivariable Controller in Response to Turbofan Engine Degradation

Jonathan S. Litt
U.S. Army Research Laboratory, Glenn Research Center, Cleveland, Ohio

Erin M. Aylward
Harvard University, Cambridge, Massachusetts

October 2003

The NASA STI Program Office . . . in Profile

Since its founding, NASA has been dedicated to the advancement of aeronautics and space science. The NASA Scientific and Technical Information (STI) Program Office plays a key part in helping NASA maintain this important role.

The NASA STI Program Office is operated by Langley Research Center, the Lead Center for NASA's scientific and technical information. The NASA STI Program Office provides access to the NASA STI Database, the largest collection of aeronautical and space science STI in the world. The Program Office is also NASA's institutional mechanism for disseminating the results of its research and development activities. These results are published by NASA in the NASA STI Report Series, which includes the following report types:

- TECHNICAL PUBLICATION. Reports of completed research or a major significant phase of research that present the results of NASA programs and include extensive data or theoretical analysis. Includes compilations of significant scientific and technical data and information deemed to be of continuing reference value. NASA's counterpart of peer-reviewed formal professional papers but has less stringent limitations on manuscript length and extent of graphic presentations.
- TECHNICAL MEMORANDUM. Scientific and technical findings that are preliminary or of specialized interest, e.g., quick release reports, working papers, and bibliographies that contain minimal annotation. Does not contain extensive analysis.
- CONTRACTOR REPORT. Scientific and technical findings by NASA-sponsored contractors and grantees.
- CONFERENCE PUBLICATION. Collected papers from scientific and technical conferences, symposia, seminars, or other meetings sponsored or cosponsored by NASA.
- SPECIAL PUBLICATION. Scientific, technical, or historical information from NASA programs, projects, and missions, often concerned with subjects having substantial public interest.
- TECHNICAL TRANSLATION. English-language translations of foreign scientific and technical material pertinent to NASA's mission.

Specialized services that complement the STI Program Office's diverse offerings include creating custom thesauri, building customized databases, organizing and publishing research results . . . even providing videos.

For more information about the NASA STI Program Office, see the following:

- Access the NASA STI Program Home Page at ***http://www.sti.nasa.gov***
- E-mail your question via the Internet to help@sti.nasa.gov
- Fax your question to the NASA Access Help Desk at 301–621–0134
- Telephone the NASA Access Help Desk at 301–621–0390
- Write to:
  NASA Access Help Desk
  NASA Center for AeroSpace Information
  7121 Standard Drive
  Hanover, MD 21076

NASA/TM—2003-212723 ARL–TR–3091

Adaptive Detuning of a Multivariable Controller in Response to Turbofan Engine Degradation

Jonathan S. Litt
U.S. Army Research Laboratory, Glenn Research Center, Cleveland, Ohio

Erin M. Aylward
Harvard University, Cambridge, Massachusetts

National Aeronautics and
Space Administration

Glenn Research Center

October 2003

Available from

NASA Center for Aerospace Information
7121 Standard Drive
Hanover, MD 21076

National Technical Information Service
5285 Port Royal Road
Springfield, VA 22100

Available electronically at http://gltrs.grc.nasa.gov

Adaptive Detuning of a Multivariable Controller in Response to Turbofan Engine Degradation

Jonathan S. Litt
U.S. Army Research Laboratory
Glenn Research Center
Cleveland, OH 44135

Erin M. Aylward
Harvard University
Cambridge, MA 02138

ABSTRACT

This paper presents an ad hoc adaptive, multivariable controller detuning rule that compensates for thrust response variations in an aircraft gas turbine engine whose performance has been degraded through use and wear. As the engine degrades the nominal thrust is no longer maintained due to a degradation-related shift in certain engine parameters. A relationship between the level of engine degradation and the deviation from the nominal thrust response was shown empirically to hold across the flight envelope and was therefore used to develop a general gain scheduled adaptive control methodology. The technique is shown to work very well in simulation up to the operability limits of the engine. Additionally, since the level of degradation can be estimated from sensor data, it would be feasible to implement the adaptive control algorithm on-line.

INTRODUCTION

Turbofan engine performance varies from engine to engine due to manufacturing tolerances and deterioration caused by use [1]. Generally the control system developed for the engine is robust enough to keep it operating within acceptable boundaries for several thousand flight cycles, even though the degradation may eventually require the engine to be overhauled as limits are reached. These limits include operability constraints such as maximum temperatures, and performance constraints such as minimum thrust response time requirements.

In most turbofan engines, thrust is regulated indirectly by controlling either Engine Pressure Ratio (EPR) or fan speed, since thrust itself can not be measured directly during flight. Although these regulated variables are maintained at their set points regardless of engine degradation, non-regulated parameters shift from their nominal values with deterioration [2]. Thus in a degraded engine, the actual thrust output, which is indirectly controlled through the regulation of other variables, may be shifted from the expected value. An option to overcome this offset in thrust is to employ a model-based control approach to provide a thrust estimate for direct control. This type of approach incorporates a simulation of the engine into the control logic that accounts for degradation-related shifts and produces an estimate of thrust, which is used for feedback. In the work presented in this paper, thrust is directly controlled using such a model-based control approach. This controller is described in a later section.

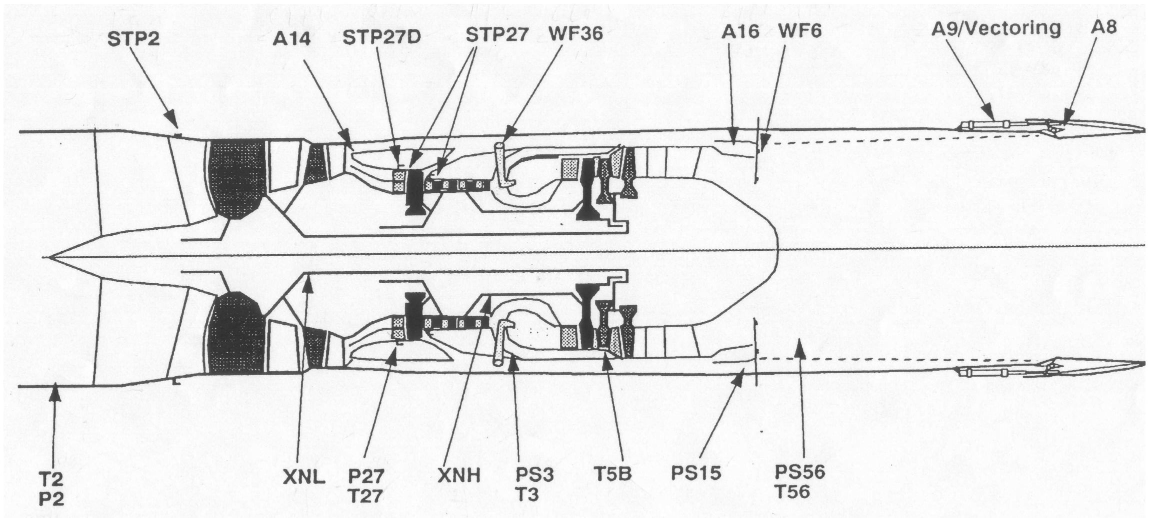

Figure 1. The MAPSS Engine

To model the performance variations mentioned above, off-nominal values of specific internal engine parameters representing major component efficiencies and flow capacities can be adjusted. These adjustment parameters are called *health parameters* [3] because they indicate the level of engine deterioration. The equations describing the degraded engine's behavior are given by

$$\begin{aligned} \dot{x}(t) &= f(x(t), u(t), p) \\ y(t) &= g(x(t), u(t), p) \end{aligned} \tag{1}$$

where x represents the engine's state vector, u the input vector, p the vector of component health parameters, and y the vector of measured outputs. When obtaining a standard linear point model of an engine, the health parameters are treated like inputs. Equation (1) may be linearized as

$$\begin{aligned} \Delta\dot{x}(t) &= A\Delta x(t) + B\Delta u(t) + L\Delta p \\ \Delta y(t) &= C\Delta x(t) + D\Delta u(t) + M\Delta p \end{aligned} \tag{2}$$

where A, B, C, D, L, and M are matrices of appropriate dimension. The Δ symbol preceding each linearized variable in equation (2) indicates the variable is a deviation from the linearization or trim point. Depending upon how the health parameters manifest themselves, the system dynamics may or may not change with degradation, but in equation (2) the state equation clearly demonstrates that steady state is only obtained when the $x(t)$ and $u(t)$ vectors shift to compensate for nonzero p. The output equation shows how nonzero values of p can produce additional steady state shifts in the output variables. In general the health parameters vary slowly enough with time that they are treated as constants in equation (2). Estimation and trending of health parameters can be achieved through a diagnostic method known as *gas path analysis*. Gas path analysis is a mathematical technique that estimates performance shifts in individual component health parameters based upon available gas path sensor measurements such as pressures, temperatures, rotor speeds, etc., and the known aero-thermodynamic relationships that exist between them [4].

Interaction of variables is normal in a multivariable control system, and the controller is designed to take advantage of the interaction to provide good closed-loop performance. Sometimes, however, one of the variables deviates from its desired value enough that it causes unacceptable disturbances in the other variables. In this case, detuning, or reducing the controller gain corresponding to that variable, may be used to effectively take that variable out of the loop and thus minimize the interaction [5]. This allows the other variables to continue to respond as intended. In this work, undesirable thrust responses due to the interaction of degraded engine variables, and an adaptive scheme to recover the nominal thrust response, are investigated using the research engine simulation Modular Aero Propulsion System Simulation MAPSS [6].

The Modular Aero Propulsion System Simulation MAPSS

The Modular Aero Propulsion System Simulation (MAPSS) model is a component level Simulink® model of a twin spool low bypass turbofan engine representative of a modern fighter aircraft engine (Figure 1). It has three state variables, three independently commanded actuators, several open-loop scheduled actuators, and multiple outputs. Additionally, the MAPSS model incorporates 10 adjustable health parameters, two for each of the five major components, for capturing the effects of degradation on the engine's performance and operability. The simulation was developed to provide a realistic public domain test bed engine model that allows access to any engine variable. Thus it is suitable for the design and evaluation of control, estimation, and diagnostic algorithms.

The MAPSS Controller

Control systems are often designed to incorporate multiple control modes, where the appropriate mode is selected based on some operability or performance criterion. This is true in flight control—for both piloted and Unmanned Air Vehicles (UAVs) [7]—and engine control [8]. In any control system, the transitions between modes should provide *bumpless transfer* [9], i.e., the transients should be smooth so that no disturbances are generated. Equation (2) implies that degradation causes shifts in the engine's trim values, and it is these shifts that can result in unacceptable behavior during mode transitions or through the violation of operability constraints.

A pseudo-model-based control approach was used to develop the MAPSS controller. In an actual model-based control implementation, estimates of unmeasurable variables such as thrust should be available to the controller through an on-board model with an associated tracking filter that estimates and updates the model health parameters to match the performance of the physical engine (Figure 2) [10]. However, because MAPSS is a simulation, all variables are available and appropriate ones are directly fed back to the controller without having to be estimated by an on-board model or tracking filter. In other words, the MAPSS simulation assumes the ideal case of perfect tracking filter performance which results in exact matching between the on-board model and the MAPSS engine. This allows control modes to be evaluated in simulation, free from implementation issues associated with an on-board model and tracking filter.

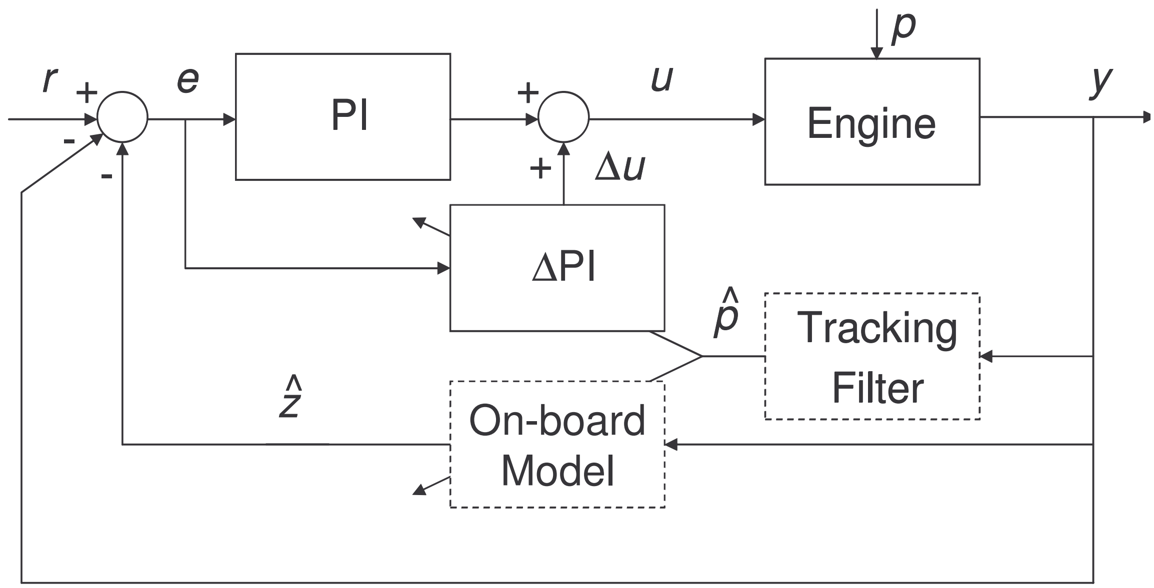

Figure 2. MAPSS adaptive controller block diagram. Dashed boxes are not currently implemented. The tracking filter block will produce an estimate $\hat{p}$ of the health parameter vector *p*. The on-board model will produce an estimate $\hat{z}$ of unmeasurable engine outputs such as thrust. PI and ΔPI are both of the form $K_P + K_I/s$ where the controller matrices are all 3×3. Note that each error signal coming into the controller is normalized using a scale factor, $SF_{variable}$

The controller in MAPSS is a multi-mode multivariable Proportional-plus-Integral (PI) controller. The performance modes are a low- and high-speed mode. The safety modes are overspeed mode and stall margin mode. Overspeed mode prevents the engine from running too fast, and stall margin mode takes over as the fan operation approaches the stall line to prevent the component from stalling. Because the low- and high-speed modes are designed for performance, safety is not explicitly accounted for in these modes because the two safety modes are blended in as needed.

In the MAPSS controller, low-speed mode is fully operational at Power Lever Angle (PLA) or throttle values below 37.5 degrees. High-speed mode is fully operational at PLA values above 42.5 degrees. In between these values the modes are blended. In low-speed mode, thrust, EPR, and LEPR (Liner Engine Pressure Ratio) are controlled; in high-speed mode, thrust, ETR (Engine Temperature Ratio), and LEPR are controlled. Each error signal coming into the controller is divided by a scale factor, $SF_{variable}$, where *variable* stands for the name of the controlled variable, such as ETR. This scaling normalizes all of the controlled variables. It will be shown later how this scale factor can be incorporated into the controller matrices as part of the adaptive scheme.

The PI gains for all modes are scheduled based on PCN2R (per cent corrected fan speed, or the fan speed as a per cent of design speed, corrected for temperature). Since all sets of gains are scheduled based on PCN2R, there is the implicit assumption that a particular value of PCN2R corresponds to a particular dynamical characterization of the engine.

The problem seen in the thrust response of the degraded MAPSS engine occurs when a throttle change moves the engine between control modes. During the low- to high-speed transition, the thrust response appears to slow down and, depending upon the level of degradation, even becomes sluggish. This response was determined to be related to the shift in engine variable values due to changes in the health parameter vector p as shown in equation (2). The health parameter term in equation (2) implies steady state shifts in both state and output variables with degradation that increase approximately linearly with increases in p. Since the controller was designed assuming a nominal engine, as the controller transitions from one mode to another, the shifted variables that are blended into the controller cause a disturbance because their contribution to the error vector is not as designed for. Even though it was not investigated, it is reasonable to expect that transitions involving the safety modes will exhibit similar deteriorated responses because different variables are blended in and out with each such transition.

Engine Performance

Although the MAPSS controller is model-based with assumed perfect tracking filter performance to account for degradation, closed-loop performance still suffers as the engine wears. The objective of this study was to make the deteriorated MAPSS engine's transient thrust response behave as much like that of a new engine as possible. This was achieved by adapting the controller as a function of degradation to recover the nominal thrust response. The underlying problem of uncontrolled variables trending toward operability limits was not addressed. For reasons of reliability and integrity, the baseline controller must be maintained intact, but an incremental control signal may be added to the baseline control signal, as in Figure 2, to improve the performance without direct alteration of the nominal control algorithm.

Modeling Deteriorated Performance Due to Usage and Aging

As an engine is used, wear occurs that degrades the engine's performance: turbine blades erode, clearances open up, etc. In order to achieve the same level of thrust as in a new engine, a deteriorated engine must run hotter and/or faster. This shift from nominal operation increases with use, and eventually reaches the point where performance can not be maintained without compromising the safety of the engine or the life of its components. The degradation in performance can be simulated by adjusting the MAPSS model component health parameters. MAPSS has 10 health parameters which include a flow capacity and efficiency scalar for the fan, low pressure compressor, high pressure compressor, high pressure turbine, and low pressure turbine.

In this work the health parameters are assumed to follow an average degradation profile over the engine's lifetime of use which consists of a fast rise into a ramp. The initial rise is intended to simulate rub-in and related new engine deterioration mechanisms [1]. As the engine ages, the health parameter degradation tends to become more linear, as shown in references [11] and [12] and Figure 3. The general empirical equation is of the form

$$p_i = a_i \cdot (1 - e^{-b_i \cdot t_{eff}}) + c_i \cdot t_{eff} \tag{3}$$

where a_i, b_i (b_i >0), and c_i are shape parameters for the i^{th} health parameter p_i. The independent variable t_{eff} represents the average time at which the given level of degradation is reached. It is measured in time or flight cycles but accounts for operating conditions that might accelerate or retard wear, i.e. t_{eff} represents the *physical age* of the engine rather than its *chronological age*; t_{eff} is sometimes called *effective cycles*. Once the initial break-in period is over, it is assumed the health parameters degrade as linear functions of t_{eff}. Thus the actual degradation p, as estimated by a tracking filter, may be used to directly calculate t_{eff} (after the initial break-in period) as

$$t_{eff} = \frac{p_i - a_i}{c_i} \tag{4}$$

It will be shown in the following sections how the estimate of t_{eff} may be used to adapt the controller on line to compensate for the effects of degradation on thrust response.

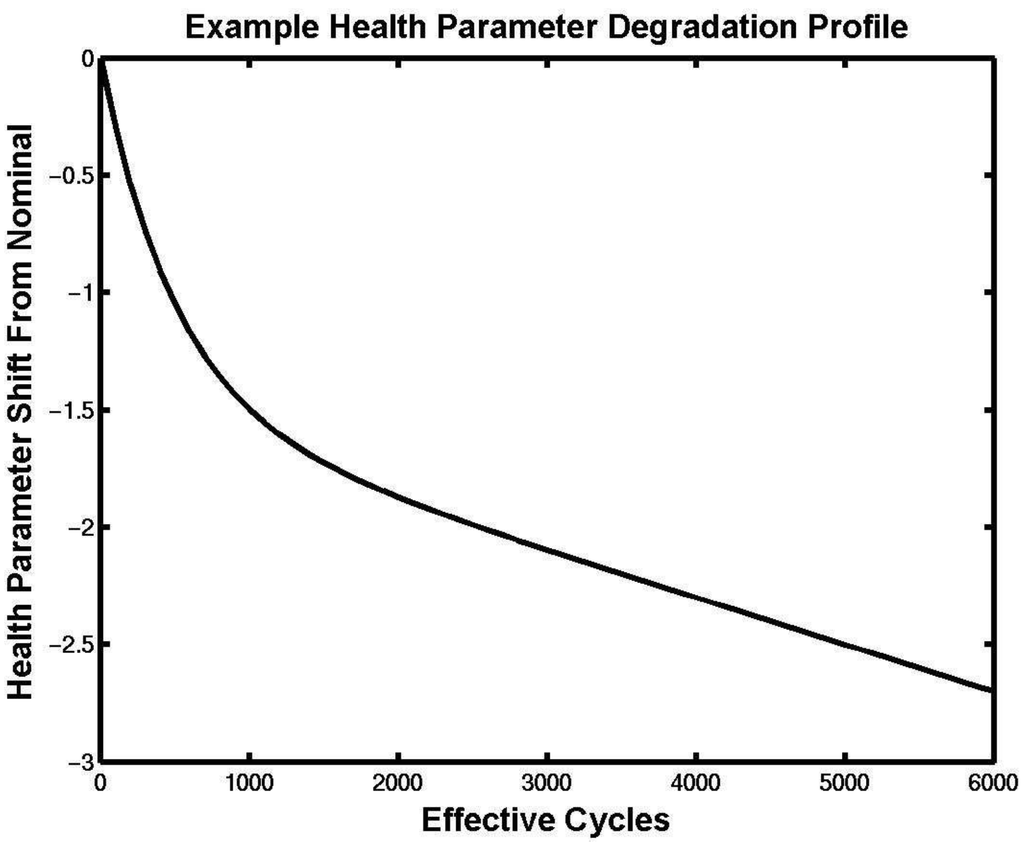

Figure 3. Typical degradation profile for a health parameter

DESCRIPTION OF THE APPROACH

It was shown in reference [13] that detuning the MAPSS engine's multivariable controller as a function of engine degradation significantly improved the thrust response for the low- to high-speed transition, which had been severely degraded by shifts in the deteriorated engine's variables. This effort modifies and extends the previous work from a single operating point to a large portion of the subsonic flight envelope. The method is further generalized to a simple detuning rule that works well within the majority of the tested region.

As previously stated, blending shifted engine variables into the controller causes the off-nominal transient thrust response. The mitigation strategy was to reduce the component of the control signal due to the excessive error in these variables to the level seen in the nominal engine. As the variables shift, the error signal entering the controller is much larger than designed for. To minimize the disruptive effect of this error on the other variables, an adaptation parameter can be computed based on engine degradation and used to scale the error so that it is brought back close to the expected level.

The flight envelope for this research was chosen to be a large portion of the entire MAPSS flight envelope. It covered most of the subsonic range, and is shown in Figure 4.

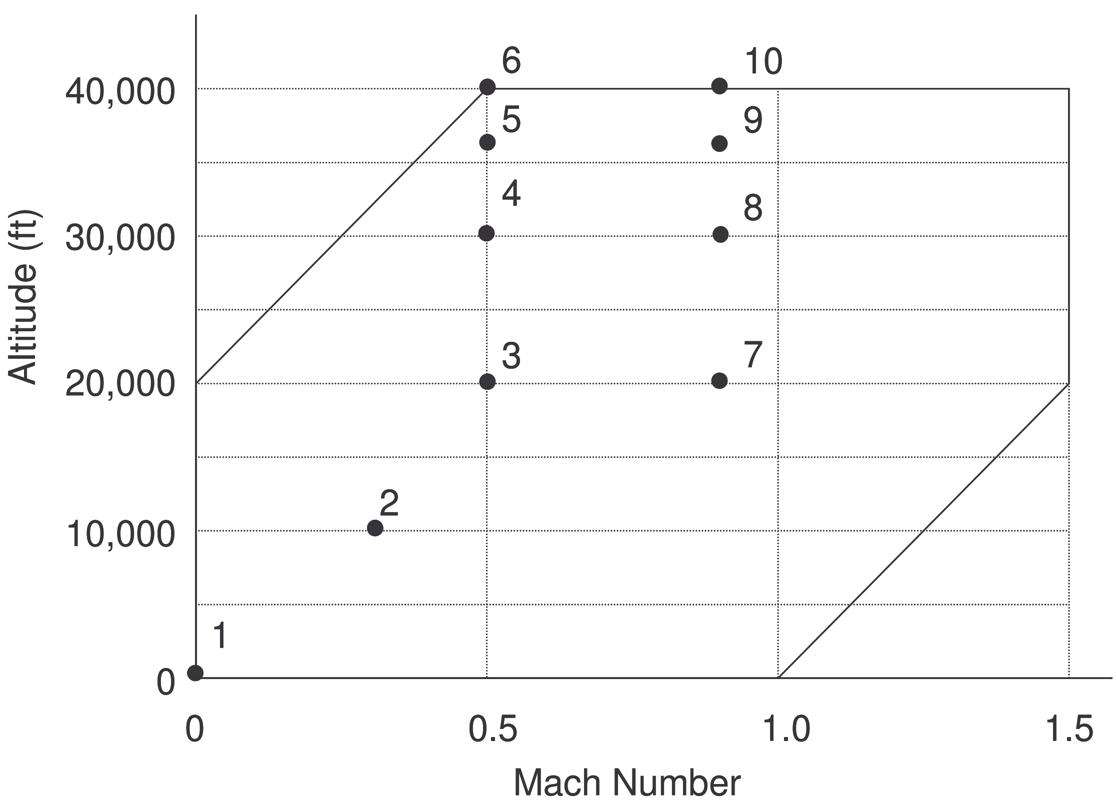

Figure 4. MAPSS test envelope used to determine adaptive control law. Test points are numbered 1-10

The test points are also listed in Table 1. The approach taken in [13] used the overshoot of the Engine Temperature Ratio (ETR) response to compute an adaptation parameter with which to tune the multivariable controller. In the current work, the technique was modified to use the ETR error response rather than the overshoot. This change was made because ETR did not overshoot at all test points, at least in the nominal case. Thus the current approach is more general.

Table 1. Test Points of the MAPSS operating envelope

Test Point	1	2	3	4	5	6	7	8	9	10
altitude feet	0K	10K	20K	30K	36,089	40K	20K	30K	36,089	40K
XN Mach number	0	0.3	0.5	0.5	0.5	0.5	0.8	0.8	0.8	0.8

The health parameter values shown in Table 2 represent shifts from the MAPSS engine's nominal values and correspond to moderate to severe degradation [1] such as might occur when the engine is due for an overhaul based on flight cycles, or when the engine is used in a particularly harsh environment such as a sandy desert or an area of volcanic activity. As shown in Table 2, the level of degradation from equation (3) in terms of effective cycles, t_{eff}, is: none, moderate (3000 cycles), heavy (4500 cycles, 1.5 times moderate), and severe (5250 cycles, 1.75 times moderate).

Table 2. Degradation values for health parameters as a change from nominal

Case	Flight Cycles	Fan		Low Pressure Compressor		High Pressure Compressor		High Pressure Turbine		Low Pressure Turbine	
	t_{eff}	η %	Flow %	η %	Flow %	η %	Flow %	η %	Flow %	η %	Flow %
0	0	0	0	0	0	0	0	0	0	0	0
1	3000	-1.5	-2.04	-1.46	-2.08	-2.94	-3.91	-2.63	1.76	-0.538	0.2588
2‡	4500	-2.18	-2.85	-2.04	-3.04	-6.17	-8.99	-3.22	2.17	-0.808	0.3407
3†	5250	-2.52	-3.25	-2.33	-3.52	-7.79	-11.53	-3.52	2.37	-0.934	0.3880
4+	6000	-2.85	-3.65	-2.61	-4.00	-9.40	-14.06	-3.81*	2.57*	-1.078*	0.4226*

‡all values in this row obtained by linear interpolation of cases 1 and 4. *extrapolated value $\eta \equiv$efficiency
†all values in this row obtained by linear interpolation of cases 2 and 4.
+this row used for linear interpolation purposes only.

Similar to the approach used in [13], the data were gathered and analyzed using the following steps:

1. Trim the nominal MAPSS engine in the low-speed mode (30° PLA). Apply a large step input to the throttle to move the engine fully into high-speed mode (48° PLA). Allow the variables to settle, and step the throttle back down to the starting point.
2. Repeat for other MAPSS engines with various levels of degradation (cases 1-3 from Table 2).
3. Plot error curves of ETR for each engine at an operating point and find the largest magnitude error that occurs during mode transition for each curve (Figure 7). Note that here error refers to reference minus feedback, *e* from Figure 2, and specifically $e_{ETR} = r_{ETR} - y_{ETR}$.

4. Compute ratio of maximum error of each degraded engine to that of the nominal engine. These adaptation parameters {α} must be positive numbers greater than 1.0. Any other numbers are unacceptable and thus the corresponding level of degradation defines the limit of the algorithm.
5. Plot the computed adaptation parameters versus degradation in terms of flight cycles t_{eff} (equation (4)) and fit a straight line through them.* The relationship between t_{eff} and the adaptation parameter α is of the general form

$$\alpha = m_{ETR} t_{eff} + b_{ETR} \tag{5}$$

so evaluating this line for the estimated level of degradation results in an adaptation parameter α for any sufficiently deteriorated MAPSS engine at the operating point.

6. Multiply the scale factor for the ETR error entering the controller by the adaptation parameter α corresponding to the level of degradation for the given engine simulation. Mathematically this is equivalent to defining ΔPI from Figure 2 as

$$\begin{aligned}\Delta \mathrm{PI}_{\text{high-speed}} &= \mathrm{PI}_{\text{high-speed}} \begin{bmatrix} 0 & 0 & 0 \\ 0 & 1 & 0 \\ 0 & 0 & 0 \end{bmatrix} \left(\frac{1}{\alpha \cdot SF_{ETR}} - \frac{1}{SF_{ETR}} \right) \\ &= \left(K_P^{high-speed} + \frac{K_I^{high-speed}}{s} \right) \begin{bmatrix} 0 & 0 & 0 \\ 0 & 1 & 0 \\ 0 & 0 & 0 \end{bmatrix} \left(\frac{1}{\alpha \cdot SF_{ETR}} - \frac{1}{SF_{ETR}} \right)\end{aligned} \tag{6}$$

In equation (6) columns of the K_P and K_I controller matrices corresponding to ETR error (the middle column of each) are rescaled from the nominal value of $1/SF_{ETR}$ =1/10 to the new value of $1/\alpha SF_{ETR}$, the adaptive scale factor. Columns corresponding to other variables or PI matrices from other control modes may be modified in a similar manner by the ΔPI controller.
7. Rerun degraded MAPSS simulation with compensated controller.
8. Repeat this procedure at points around the operating envelope.
9. Fit a surface to the lines found in step 5 as a function of altitude and Mach number, i.e. determine a function to calculate the value of the slope and intercept of the adaptation parameter line as a function of altitude and Mach number.

* It was shown in [13] that the adaptation parameter varies linearly with degradation. Even though this work uses ETR error rather that ETR overshoot to compute the adaptation parameter the straight line approximation still holds.

RESULTS

Figure 5 and Figure 6 show representative responses in ETR and EPR to a PLA change from low- to high-speed mode and high- to low-speed mode, respectively. The corresponding error plots are shown in Figure 7 and Figure 8, respectively. In low-speed mode, EPR is controlled to a set point while ETR floats, but in high-speed mode the opposite is true. It is clear from the figures that EPR decreases and ETR increases with degradation when they are not under control. The increase in ETR represents the general operating temperature increase in engines with deterioration.

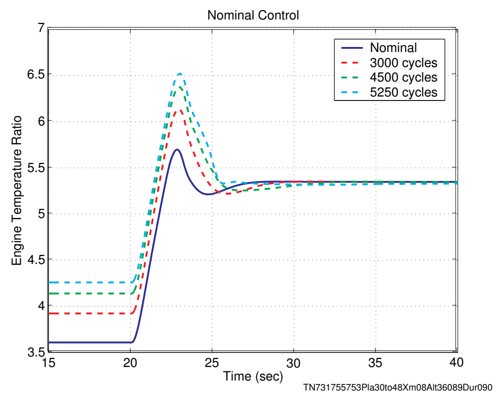

Figure 5. Representative ETR responses for a set of degraded engines with nominal control during low- to high-speed mode transition

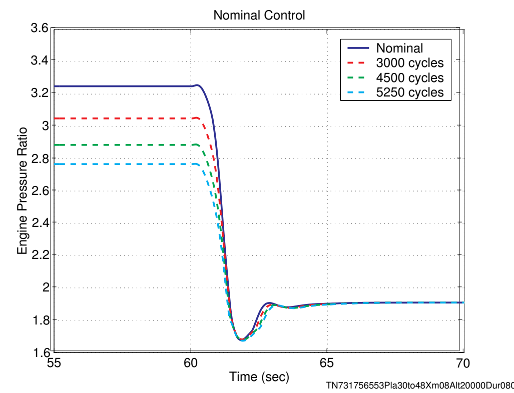

Figure 6. Representative EPR responses for a set of degraded engines with nominal control during high- to low-speed mode transition

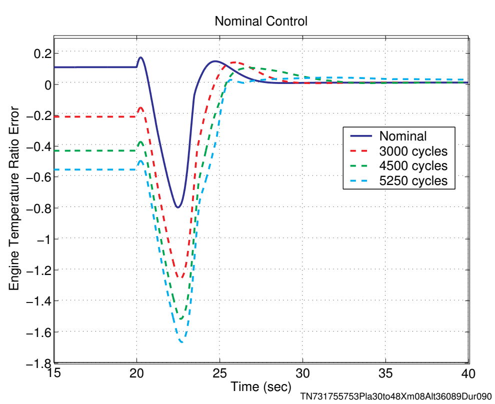

Figure 7. Representative ETR error responses for a set of degraded engines with nominal control during low- to high-speed mode transition

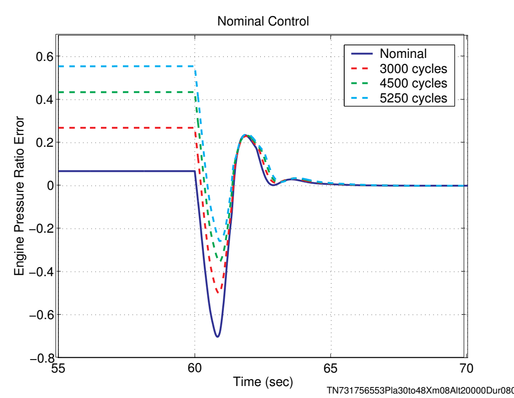

Figure 8. Representative EPR error responses for a set of degraded engines with nominal control during high- to low-speed mode transition

The transition from low- to high-speed mode was evaluated following the approach listed in the previous section for the operating points in Figure 4. The results are shown in Figure 9 through Figure 18. The results varied, but in all cases the thrust responses obtained using the compensated controller showed improvement over the responses of the degraded engines with nominal control.

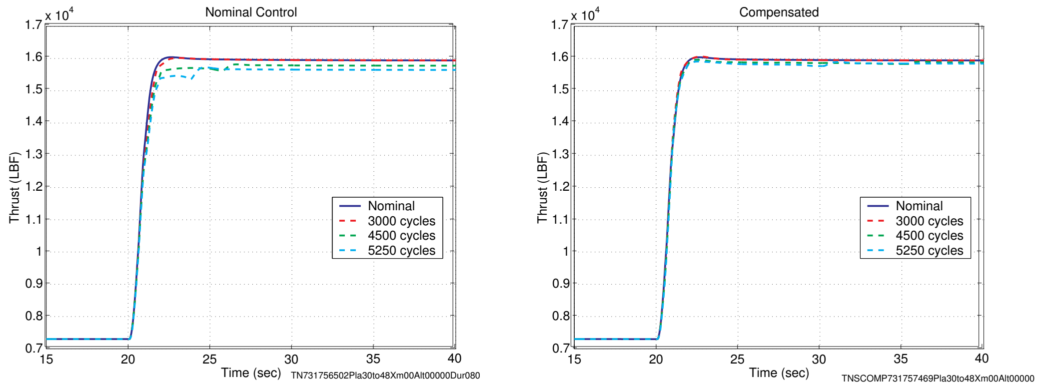

Figure 9. Nominal and compensated thrust responses for a set of degraded engines at test point 1, 0 ft, Mach 0.0

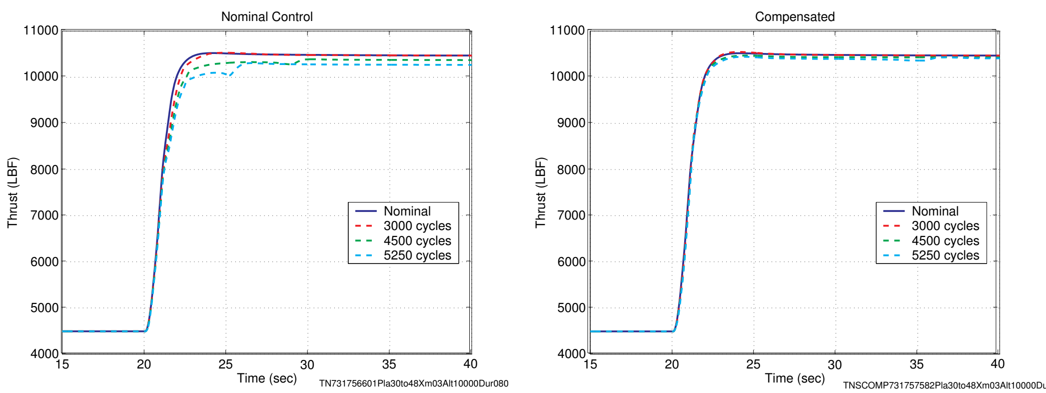

Figure 10. Nominal and compensated thrust responses for a set of degraded engines at test point 2, 10,000 ft, Mach 0.3

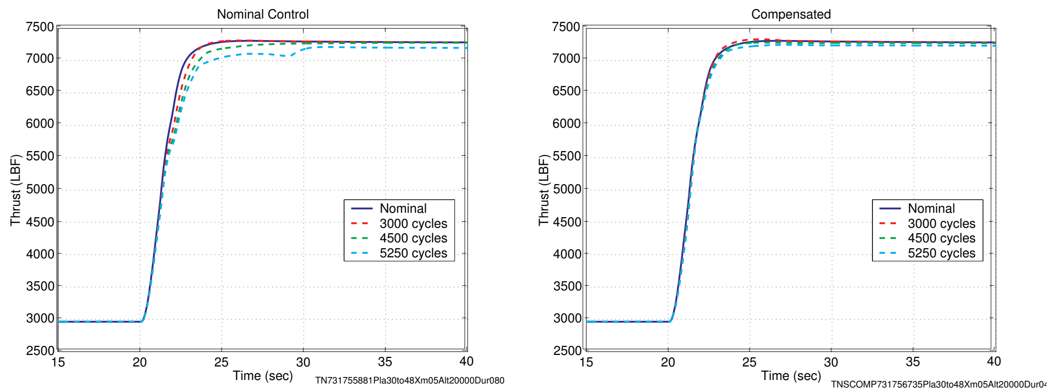

Figure 11. Nominal and compensated thrust responses for a set of degraded engines at test point 3, 20,000 ft, Mach 0.5

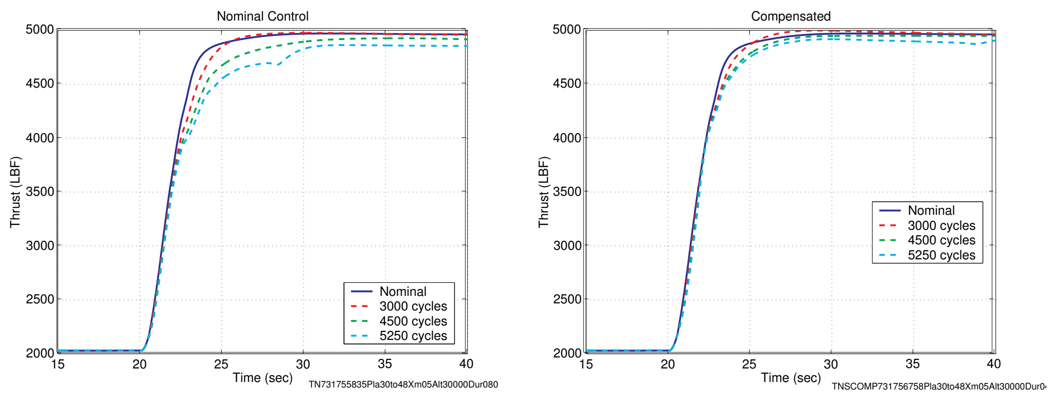

Figure 12. Nominal and compensated thrust responses for a set of degraded engines at test point 4, 30,000 ft, Mach 0.5

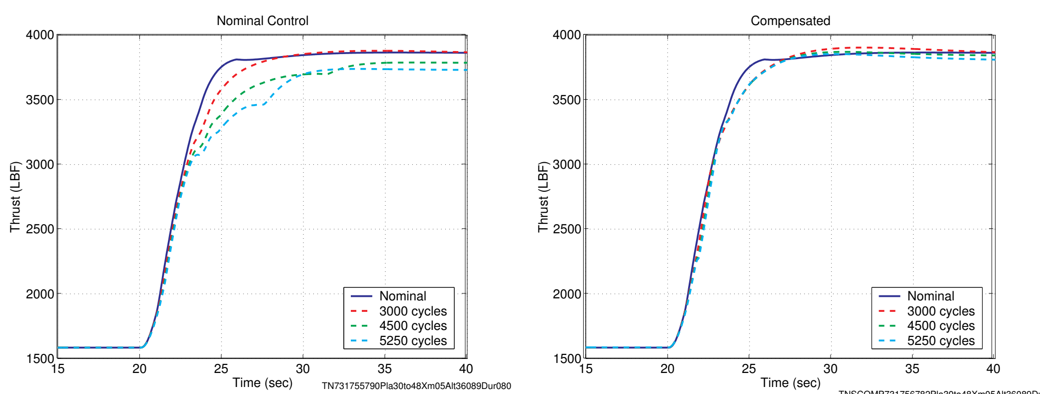

Figure 13. Nominal and compensated thrust responses for a set of degraded engines at test point 5, 36,089 ft, Mach 0.5

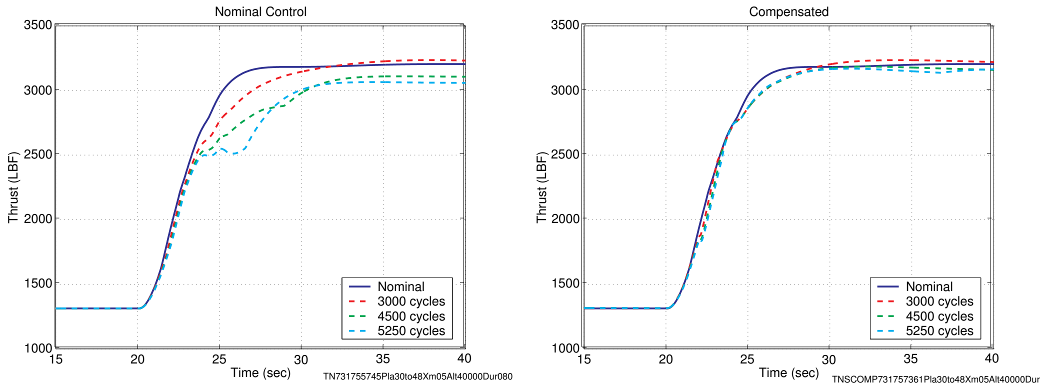

Figure 14. Nominal and compensated thrust responses for a set of degraded engines at test point 6, 40,000 ft, Mach 0.5

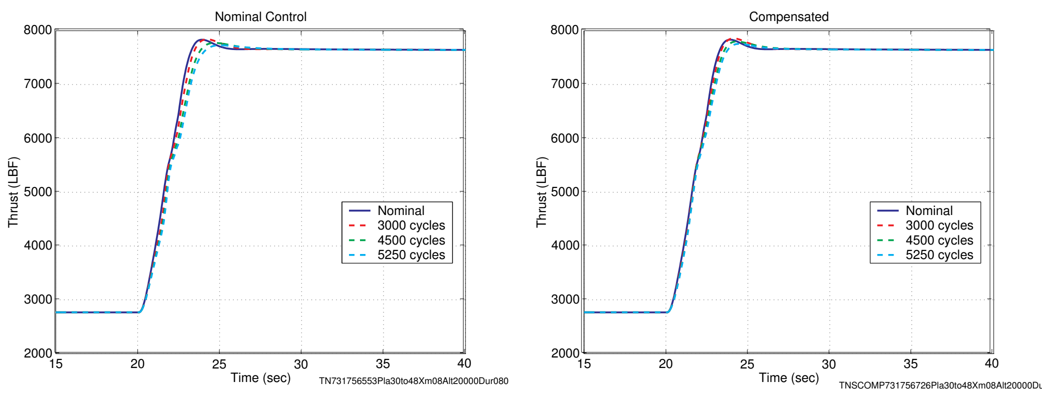

Figure 15. Nominal and compensated thrust responses for a set of degraded engines at test point 7, 20,000 ft, Mach 0.8

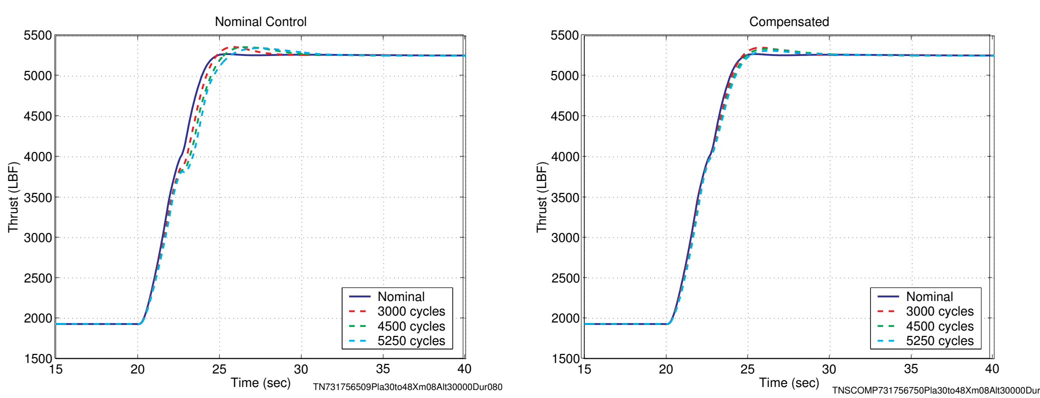

Figure 16. Nominal and compensated thrust responses for a set of degraded engines at test point 8, 30,000 ft, Mach 0.8

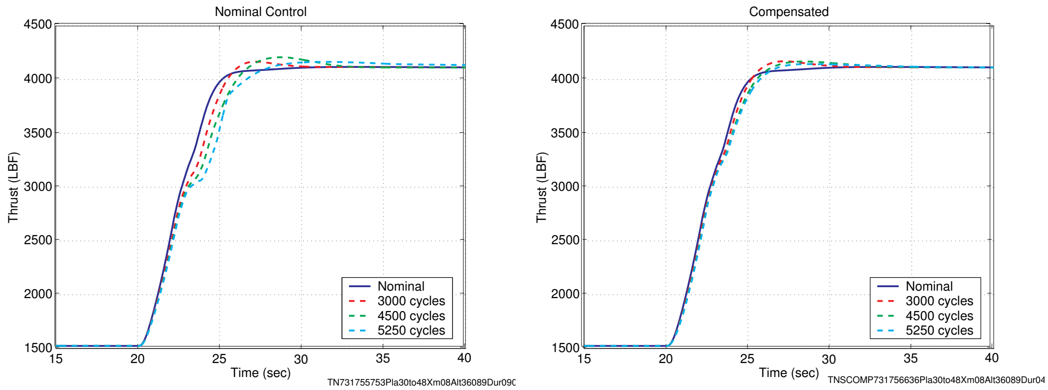

Figure 17. Nominal and compensated thrust responses for a set of degraded engines at test point 9, 36,089 ft, Mach 0.8

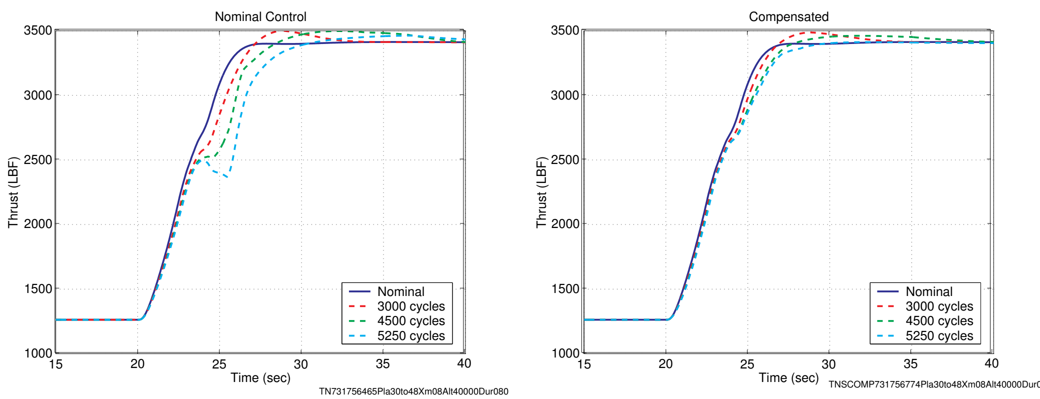

Figure 18. Nominal and compensated thrust responses for a set of degraded engines at test point 10, 40,000 ft, Mach 0.8

Representative values of other engine variables (Figure 19 through Figure 23) confirm what was demonstrated in [13]: the other variables settle to the same values as their nominal control counterparts with generally smoother responses, i.e., transient response is improved in the compensated case while steady state values are unaffected. This means that the approach used to improve the thrust performance will recover the transient response but will not protect the engine from operating hotter and faster up to the allowable limits to produce the requested thrust as the engine ages.

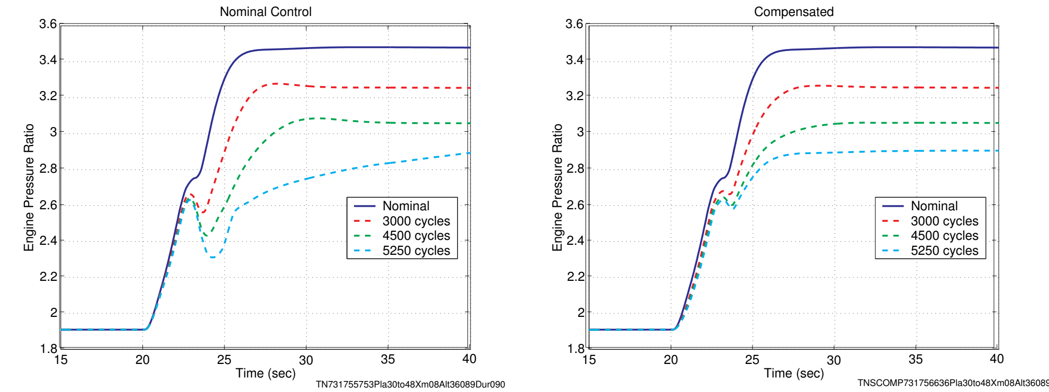

Figure 19. Nominal and compensated EPR responses for a set of degraded engines at test point 9, 36,089 ft, Mach 0.8

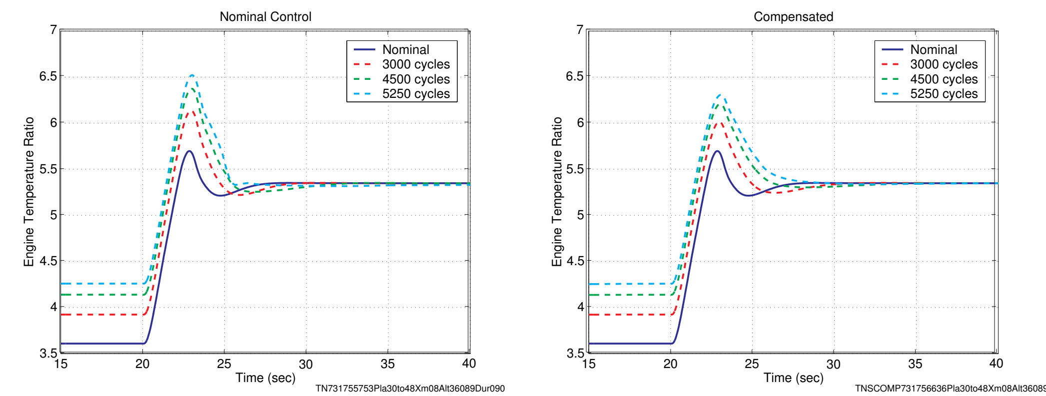

Figure 20. Nominal and compensated ETR responses for a set of degraded engines at test point 9, 36,089 ft, Mach 0.8

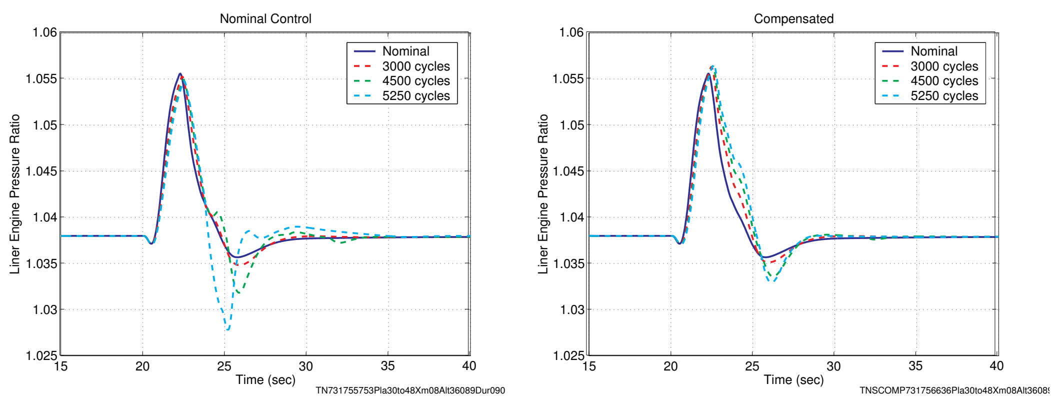

Figure 21. Nominal and compensated LEPR responses for a set of degraded engines at test point 9, 36,089 ft, Mach 0.8

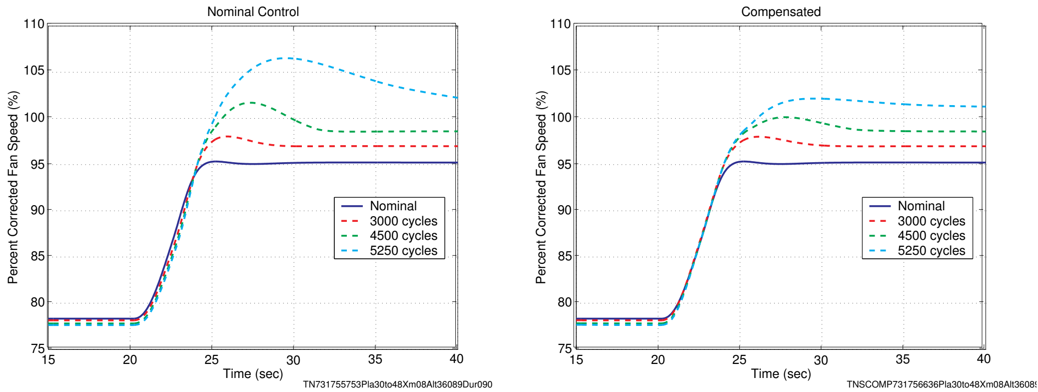

Figure 22. Nominal and compensated PCN2R responses for a set of degraded engines at test point 9, 36,089 ft, Mach 0.8

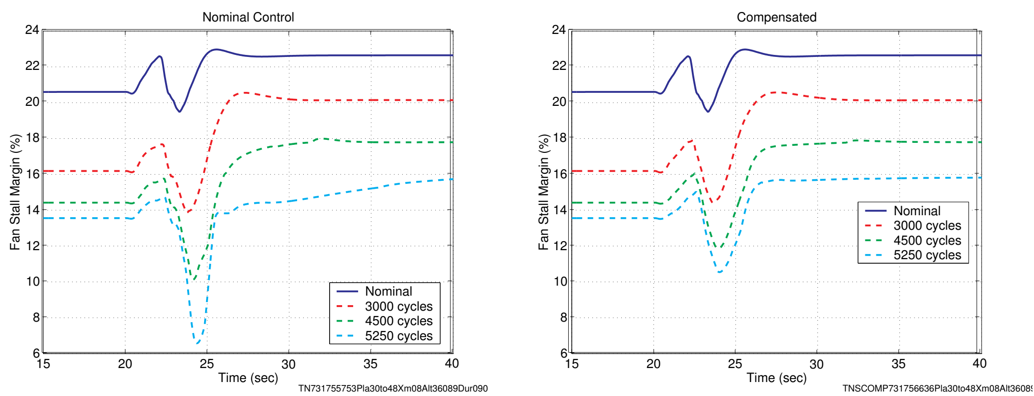

Figure 23. Nominal and compensated Fan stall margin responses for a set of degraded engines at test point 9, 36,089 ft, Mach 0.8

Figure 24 shows the adaptation parameters calculated using the ETR error ratios at the selected levels of degradation for each test point. Notice that all but test point 5 (36,089 ft, Mach 0.5) are reasonably linear. Straight line approximations of adaptation parameter vs. t_{eff} were fit to the calculated adaptation parameter values determined at each test point. Surfaces were then fit to the slopes m (Figure 25) and intercepts b (Figure 26) of these lines to provide a general rule for computing an adaptation parameter line as a function of altitude and Mach number. The slopes calculated at each test point fit relatively well on a plane except for points 1, 5, and 6. Without any insight into what sort of shape the surfaces should be, rather than try to use a complicated shape to fit all points, planes were used with points 1, 5, and 6 removed. The resulting planes from equation (5) are described by the following equations

$$m_{ETR} = 8.867\times10^{-4} - 1.034\times10^{-3}\cdot XN + 3.654\times10^{-9}\cdot altitude$$

$$b_{ETR} = 8.184\times10^{-1} + 2.396\times10^{-1}\cdot XN - 7.140\times10^{-7}\cdot altitude$$

where *XN* is Mach number and *altitude* is in feet. The percent error between each slope *m* and intercept *b* value used in the surface fit and its planar approximation appears in Table 3. The largest errors in slope correspond to the least steep slopes, where a small difference may still be a large percentage of the true value. Since a small value for slope corresponds to a small change in α over the range of degradation, even a large percent error in slope results in only a small total error in α.

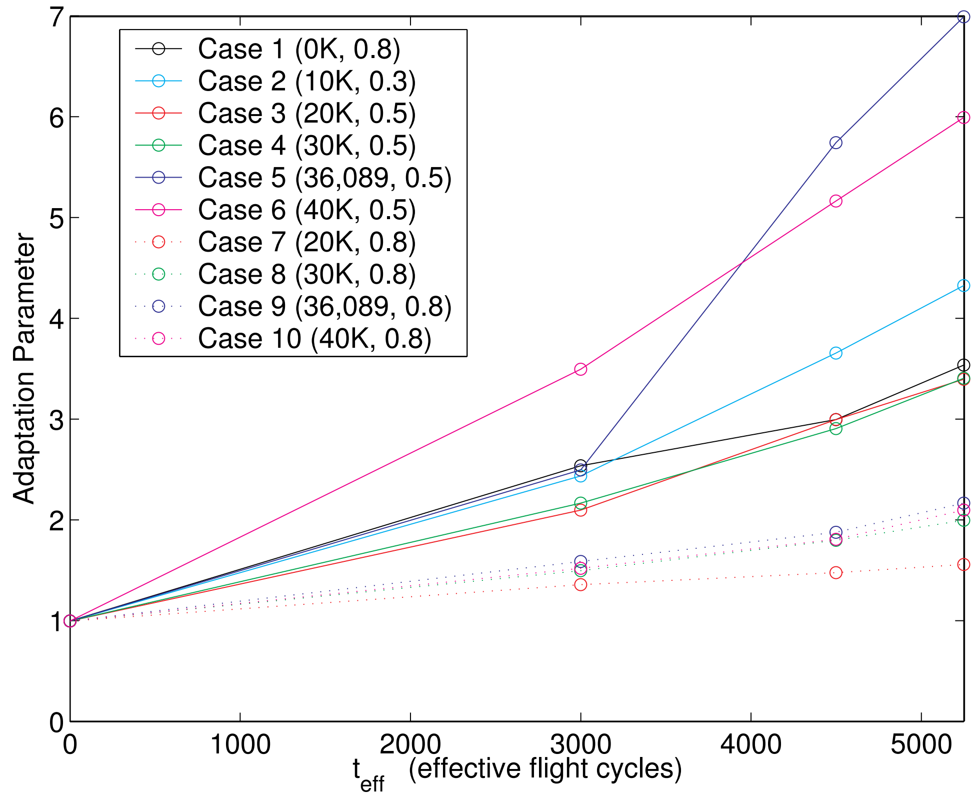

Figure 24. Adaptation parameters vs. effective flight cycles for degraded engines at the test points

Table 3. Percent error magnitude for each test point's slope and intercept using a planar fit

Test Point	2	3	4	7	8	9	10
Slope error	1.7%	2.8%	6.8%	25%	9.3%	10.4%	2.9%
Intercept error	1.6%	0.14%	2.7%	1.5%	0.89%	0.59%	1.1%

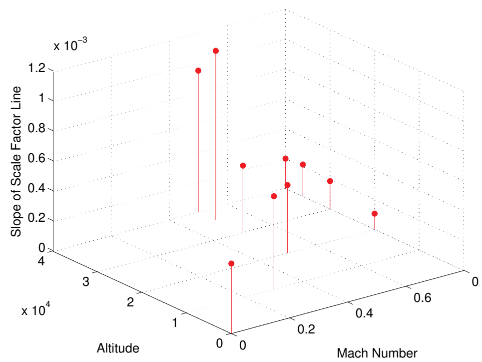

Figure 25. Adaptation parameter slopes based on least squares line fits for the ten test points

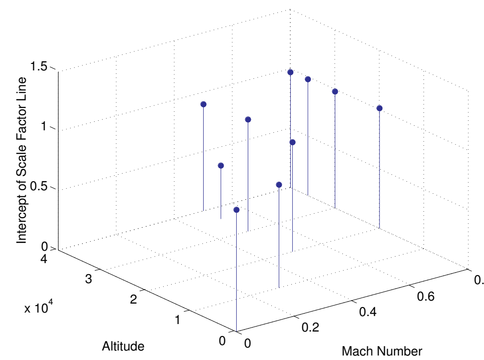

Figure 26. Adaptation parameter intercepts based on least squares line fits for the ten test points

The fitted surface was next used to compute adaptation parameters at an intermediate validation point, altitude 35,000 ft, Mach 0.65. Figure 27 shows levels of improvement similar to the test cases.

The error metric used to measure the thrust recovery was the maximum instantaneous absolute difference between the nominal and the compensated response. This metric indicates how closely the compensated response recovers the nominal thrust performance at any point in time. To obtain the maximum instantaneous percent difference, the maximum difference between the responses was divided by the net change in thrust due to the throttle input. It should be noted that the instantaneous difference depends strongly on the adaptation parameter which in turn depends on the method used to determine it. This is demonstrated by comparing the results in [13] using the ETR overshoot method (Figure 28) to those shown here using the ETR error method (Figure 17). This indicates that there is some arbitrariness in the adaptation parameter computation that allows for more conservative or aggressive compensation, which directly relates to the matching of the responses.

The percentage maximum instantaneous difference between each nominal response and its compensated case is given in Table 4.

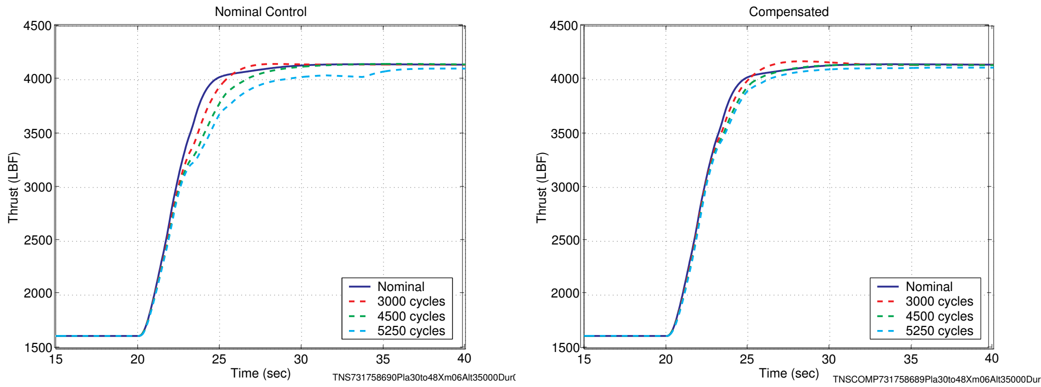

Figure 27. Nominal and compensated thrust responses for a set of degraded engines at validation point 35,000 ft, Mach 0.65

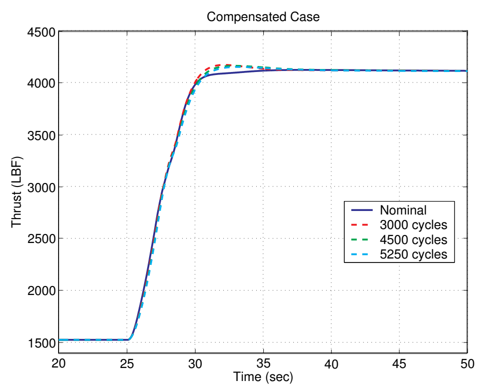

Figure 28. Thrust responses for a set of degraded engines using the ETR overshoot compensation method at test point 9, 36,089 ft, Mach 0.8

Table 4. Maximum instantaneous absolute difference between nominal thrust response and compensated degraded thrust response divided by total net change in thrust due to throttle input

Error / Test Point	% of nominal for 3000 cycles	% of nominal for 4500 cycles	% of nominal for 5250 cycles
1	3.02%	3.10%	3.97%
2	2.26%	4.00%	5.13%
3	2.88%	4.27%	4.95%
4	5.01%	6.83%	7.35%
5	6.78%	8.14%	9.57%
6	5.85%	8.93%	10.53%
7	3.04%	6.49%	9.15%
8	3.06%	5.10%	6.19%
9	3.83%	6.54%	7.57%
10	5.25%	9.20%	10.75%
Validation point	4.01%	7.06%	8.91%

The step down from high- to low-speed mode showed a different characteristic. First of all the magnitude of the Engine Pressure Ratio (EPR) error during the transition was consistently less with degradation than in the nominal case. Using the algorithm described above to obtain the adaptation parameters would have led to ratios less than 1.0, which implies an amplification of the EPR error rather than the attenuation that takes place in the ETR error (low- to high-speed) case. In general it is destabilizing to increase loop gains [5] and doing so blindly is strongly cautioned against. However, the thrust responses of the degraded engines with nominal controllers were similar to the nominal response in each case as long as the degradation was not too severe (Figure 29 through Figure 38). Test points 7 through 10 show closely matching responses for all levels of degradation, while test points 1 through 6 show severe deterioration in the thrust response as EPR error increases past a critical level. This sudden break from good to unacceptable transient behavior is characterized by a severe oscillation disturbance in the thrust response, delineating an operability limit corresponding to a level of degradation. It occurs once the degradation-induced shift raises EPR enough that the EPR error remains positive during the control mode transition.

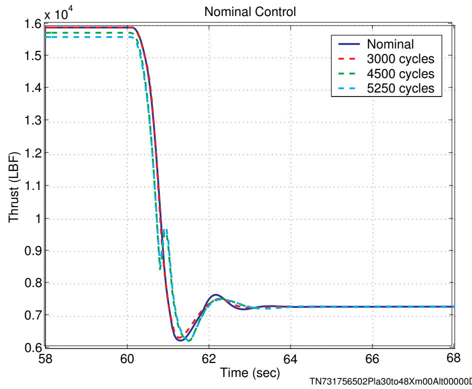

Figure 29. Thrust responses for a set of degraded engines with nominal control at test point 1, 0 ft, Mach 0.0

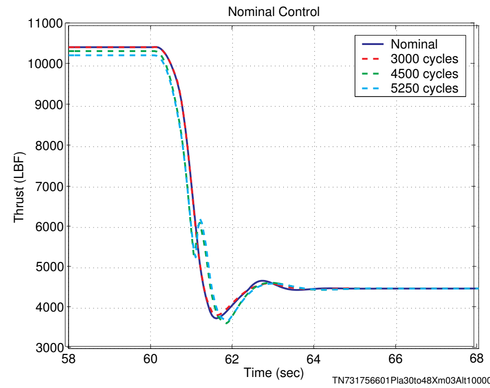

Figure 30. Thrust responses for a set of degraded engines with nominal control at test point 2, 10,000 ft, Mach 0.3

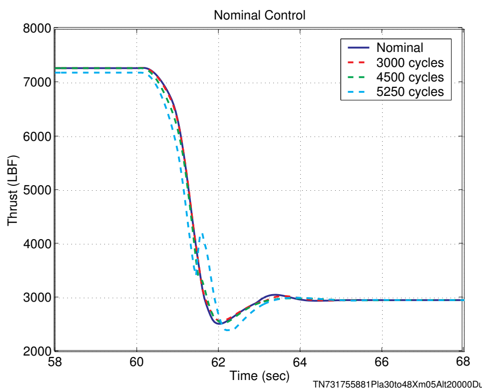

Figure 31. Thrust responses for a set of degraded engines with nominal control at test point 3, 20,000 ft, Mach 0.5

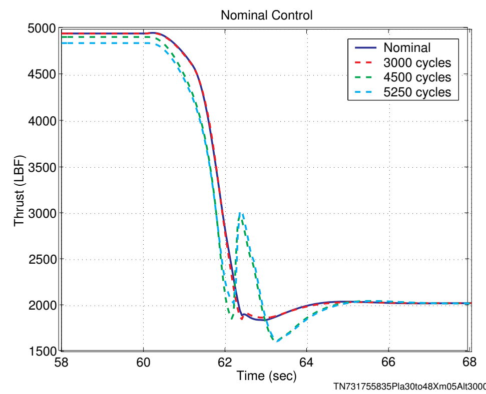

Figure 32. Thrust responses for a set of degraded engines with nominal control at test point 4, 30,000 ft, Mach 0.5

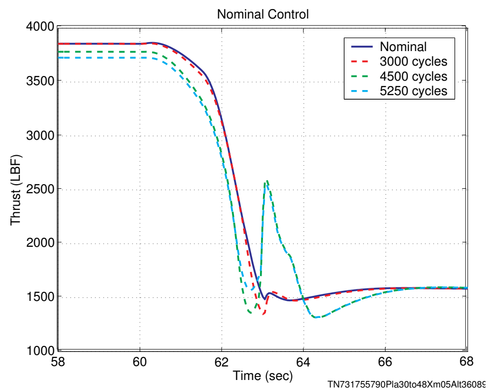

Figure 33. Thrust responses for a set of degraded engines with nominal control at test point 5, 36,089 ft, Mach 0.5

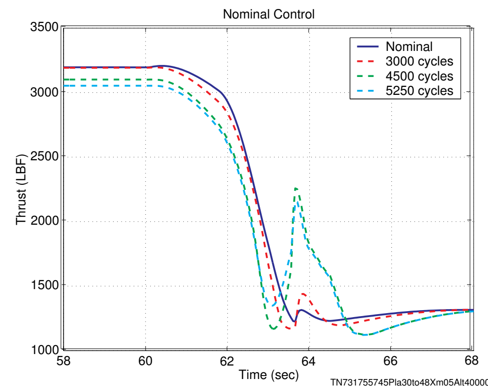

Figure 34. Thrust responses for a set of degraded engines with nominal control at test point 6, 40,000 ft, Mach 0.5

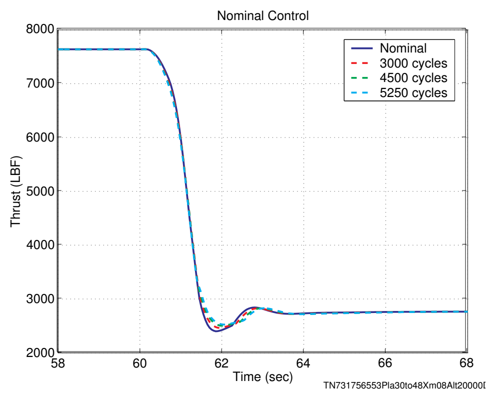

Figure 35. Thrust responses for a set of degraded engines with nominal control at test point 7, 20,000 ft, Mach 0.8

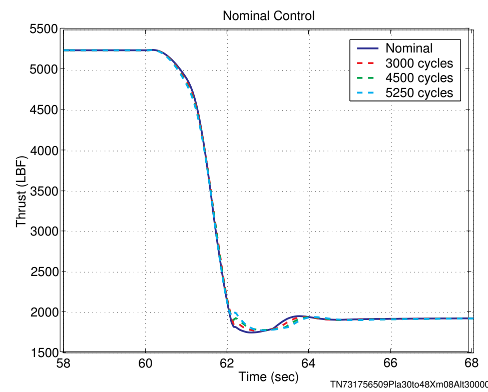

Figure 36. Thrust responses for a set of degraded engines with nominal control at test point 8, 30,000 ft, Mach 0.8

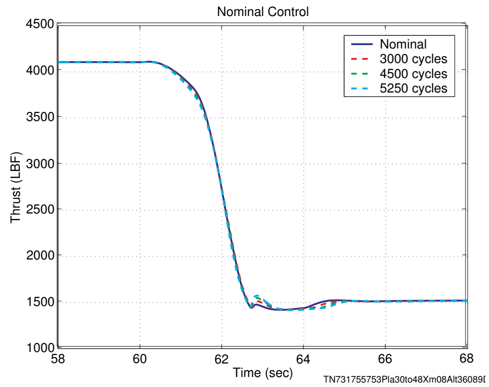

Figure 37. Thrust responses for a set of degraded engines with nominal control at test point 9, 36,089 ft, Mach 0.8

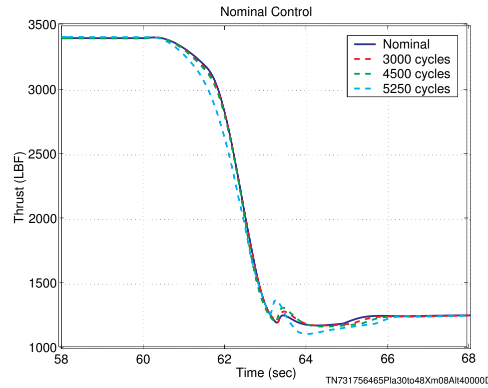

Figure 38. Thrust responses for a set of degraded engines with nominal control at test point 10, 40,000 ft, Mach 0.8

The relationship of the EPR shift to the oscillation during the transient is plainly demonstrated in Figure 39. This transient is clearly a candidate for detuning since the thrust response is devastatingly upset by the oscillations in EPR error; however a rule for the detuning is not as readily apparent as it was for the case where an increase in thrust is requested. Thus no controller adaptation rule was identified for the downward transient, but it is recommended that one be developed or other techniques be investigated for use in these situations. For reference, Figure 40 shows the detuned highly degraded (5250 cycles) thrust response at test point 5 (36,089 feet, Mach 0.5), Figure 41 shows the corresponding EPR plots and Figure 42 shows the EPR error plots. There is improvement as the controller is detuned, but from looking at Figure 33, Figure 39, Figure 40, and Figure 42, it is clear that detuning is only required once the EPR error shifts enough in a positive direction. However, there is no obvious way to obtain the adaptation parameter except by trial and error.

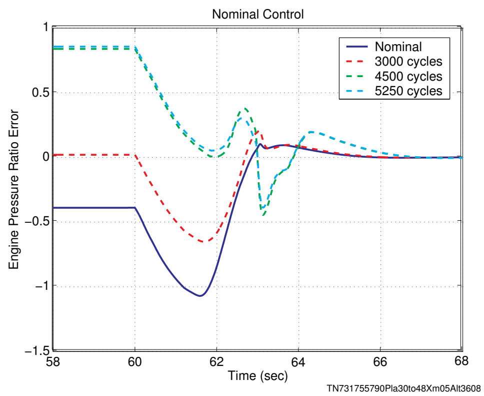

Figure 39. EPR error for a set of degraded engines with nominal control at test point 5, 36,089 ft, Mach 0.5

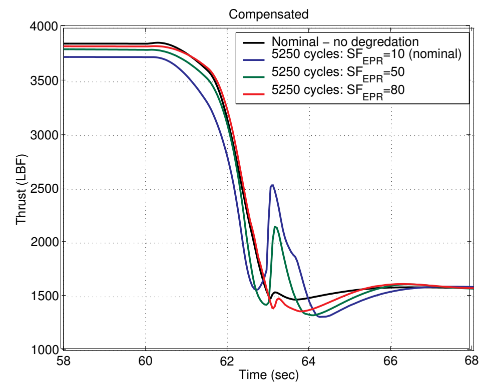

Figure 40. Thrust response for a highly degraded engine with various amounts of compensation at test point 5, 36,089 ft, Mach 0.5

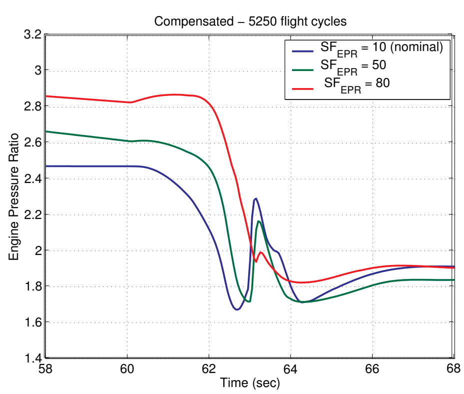

Figure 41. EPR response for a highly degraded engine with various amounts of compensation at test point 5, 36,089 ft, Mach 0.5

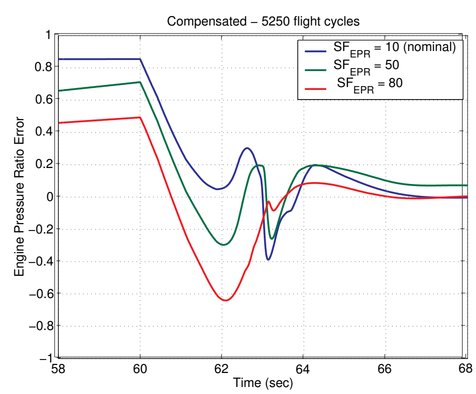

Figure 42. EPR error for a highly degraded engine with various amounts of compensation at test point 5, 36,089 ft, Mach 0.5

CONCLUSIONS

The simple detuning rule demonstrated here in simulation for an increase in thrust demand worked well across a large portion of the flight envelope, and could easily be modified to cover the entire tested region. The controller adaptation effectively smoothes the mode blending and maintains the nominal thrust response over a range of degradation. This means that the degraded thrust response will not be a cause for removal of the engine, thus possibly extending on-wing life. Detuning was also shown to work in the case where the thrust demand was decreased, but no simple rule was developed to adapt the controller. More work needs to be done in this area to develop a general methodology to achieve a smooth downward thrust transient, otherwise successful compensation in the upward direction is of limited value. Overall the results are promising that mode switching multivariable PI controllers can be adaptively detuned to maintain performance of severely deteriorated engines. Since bumpless transfer is a requirement for mode switching controllers, this becomes critical as the engine ages.

More work still needs to be done to evaluate the robustness of the scheme to off-nominal degradation trajectories. It is also important to identify which health parameters have the most impact on the degraded response, since the technique may be insensitive to variations in some parameters but not others. This implies that for the correct computation of α, the determination of t_{eff} in equation (4) may depend on a specific subset of heath parameters which has yet to be determined.

Once a tracking filter is developed, the algorithm can be tested under more realistic conditions, with estimated health parameters and model-based estimates used for feedback. Since the health parameters are assumed to vary slowly, good estimation should result in steady, consistent values of α as functions of altitude, Mach number, and degradation. However the issue of implementing the tracking filter and on-board model is not trivial.

REFERENCES

1. Sallee, G. P., "Performance Deterioration Based on Existing (Historical) Data; JT9D Jet Engine Diagnostics Program," NASA Contractor Report 135448, 1978.

2. Mattingly, Jack, Elements of Gas Turbine Propulsion, McGraw-Hill, 1996.

3. Kobayashi, T.; Simon, D. L., "A Hybrid Neural Network-Genetic Algorithm Technique for Aircraft Engine Performance Diagnostics," 37th Joint Propulsion Conference and Exhibit, Salt Lake City, UT, July 8-11, 2001.

4. Urban, L. A., "Gas Path Analysis Applied to Turbine Engine Condition Monitoring," AIAA/SAE 8th Joint Propulsion Specialist Conference, November 29-December 1, 1972, New Orleans, LA, AIAA Paper No. 72-1082.

5. Murrill, P. W., Application Concepts of Process Control, Instrument Society of America, 1988.

6. Parker, K. I., Guo, T. H., “Development of a Turbofan Engine Simulation in a Graphical Simulation Environment,” NASA/TM—2003-212543.

7. Gutiérrez, L. B., Vachtsevanos, G., Heck, B., “An Approach to the Adaptive Mode Transition Control of Unmanned Aerial Vehicles,” Proceedings of the American Control Conference, Denver, CO, June 4-6, 2003.

8. Nobbs, S. G., Jacobs, S. W., Donahue, D. J., “Development of the Full-Envelope Performance Seeking Control Algorithm,” 28th Joint Propulsion Conference and Exhibit, Nashville, TN, July 6-8, 1992, AIAA 92-3748.

9. Astrom, K. J., Wittenmark, B. J., Computer-Controlled Systems: Theory and Design, 3rd Edition, Prentice Hall, 1997.

10. Shaw, P.; Foxgrover, J.; Berg, D. F., Swan, J.; Adibhatla, S.; Skira, C. A., “A Design Approach to a Performance Seeking Control,” AIAA/ASME/SAE/ASEE 22nd Joint Propulsion Conference, Huntsville, AL, June 16-18, 1986, AIAA-86-1674.

11. Sasahara, O., “JT9D Engine/Module Performance Deterioration Results from Back to Back Testing,” ISABE 85-7061, Seventh International Symposium on Air Breathing Engines, Beijing, PRC, September 2-6, 1985.

12. Simon, D.; Simon, D.L., “Aircraft Turbofan Engine Health Estimation Using Constrained Kalman Filtering,” ASME-GT2003-38584, International Gas Turbine and Aeroengine Congress and Exposition, Atlanta, GA, June 2003.

13. Litt, J. S.; Parker, K. I.; Chatterjee, S., “Adaptive Gas Turbine Engine Control for Deterioration Compensation Due to Aging,” 16th International Symposium on Air Breathing Engines, Cleveland, OH, August 31-September 5, 2003, ISABE 2003-1056.

REPORT DOCUMENTATION PAGE

Form Approved
OMB No. 0704-0188

1. AGENCY USE ONLY (*Leave blank*)	2. REPORT DATE	3. REPORT TYPE AND DATES COVERED
	October 2003	Technical Memorandum

4. TITLE AND SUBTITLE

Adaptive Detuning of a Multivariable Controller in Response to Turbofan Engine Degradation

5. FUNDING NUMBERS

WBS–22–704–04–03
1L161102AF20

6. AUTHOR(S)

Jonathan S. Litt and Erin M. Aylward

7. PERFORMING ORGANIZATION NAME(S) AND ADDRESS(ES)

National Aeronautics and Space Administration
John H. Glenn Research Center at Lewis Field
Cleveland, Ohio 44135–3191

8. PERFORMING ORGANIZATION REPORT NUMBER

E–14247

9. SPONSORING/MONITORING AGENCY NAME(S) AND ADDRESS(ES)

National Aeronautics and Space Administration
Washington, DC 20546–0001
and
U.S. Army Research Laboratory
Adelphi, Maryland 20783–1145

10. SPONSORING/MONITORING AGENCY REPORT NUMBER

NASA TM—2003-212723
ARL–TR–3091

11. SUPPLEMENTARY NOTES

Jonathan S. Litt, U.S. Army Research Laboratory, Glenn Research Center, and Erin M. Aylward, Harvard University, Cambridge, Massachusetts 02138. Responsible person, Jonathan S. Litt, organization code 0300, 216–433–3748.

12a. DISTRIBUTION/AVAILABILITY STATEMENT

Unclassified - Unlimited
Subject Category: 07 Distribution: Nonstandard

Available electronically at http://gltrs.grc.nasa.gov

This publication is available from the NASA Center for AeroSpace Information, 301–621–0390.

12b. DISTRIBUTION CODE

13. ABSTRACT ***(Maximum 200 words)***

This paper presents an ad hoc adaptive, multivariable controller detuning rule that compensates for thrust response variations in an aircraft gas turbine engine whose performance has been degraded through use and wear. As the engine degrades, the nominal thrust is no longer maintained due to a degradation-related shift in certain engine parameters. A relationship between the level of engine degradation and the deviation from the nominal thrust response was shown empirically to hold across the flight envelope and was therefore used to develop a general gain scheduled adaptive control methodology. The technique is shown to work very well in simulation up to the operability limits of the engine. Additionally, since the level of degradation can be estimated from sensor data, it would be feasible to implement the adaptive control algorithm on-line.

14. SUBJECT TERMS

Adaptive control; Propulsion; Engine degradation

15. NUMBER OF PAGES

32

16. PRICE CODE

17. SECURITY CLASSIFICATION OF REPORT	18. SECURITY CLASSIFICATION OF THIS PAGE	19. SECURITY CLASSIFICATION OF ABSTRACT	20. LIMITATION OF ABSTRACT
Unclassified	Unclassified	Unclassified	